



## Effect of Solid Particle Properties on Heat Transfer and Pressure Drop in Packed Duct

Kifah H. Hilal

Salman H. Omran

Muthanna L. Abdulla

Department of Mechanical/ Institute of Technology- Baghdad

(Received 3 October 2012; Accepted 30 April 2013)

### Abstract

This work examines numerically the effects of particle size, particle thermal conductivity and inlet velocity of forced convection heat transfer in uniformly heated packed duct. Four packing material (Aluminum, Alumina, Glass and Nylon) with range of thermal conductivity (from 200 W/m.K for Aluminum to 0.23 W/m.K for Nylon), four particle diameters (1, 3, 5 and 7 cm), inlet velocity (0.07, 0.19 and 0.32 m/s) and constant heat flux (1000, 2000 and 3000 W/m<sup>2</sup>) were investigated. Results showed that heat transfer (average Nusselt number  $Nu_{av}$ ) increased with increasing packing conductivity; inlet velocity and heat flux, but decreased with increasing particle size. Also, Aluminum average Nusselt number is about (0.85, 2.2 and 3.1 times) than Alumina, glass and Nylon respectively. From optimization between heat transfer and pressure drop through packed duct, it is found that finest ratio ( $Nu_{av} / \Delta p$ ) equal to (19.12) at ( $D_p = 7$  cm, inlet velocity = 0.07 m/s and 3000 W/m<sup>2</sup> heat flux) with Aluminum as packing material.

**Keywords:** sphere particle, packed duct, heat transfer.

### 1. Introduction

Packed beds used in many applications in the industry ranging from heat and phase exchangers to heterogeneous catalytic reactors. Packed bed equipment often consist of a tubular shell filled with solid pellets or particles such as conductive metal pellets in heat exchangers, catalytic porous media in catalytic reactors or, in the case of phase exchangers, plastic or ceramic packing material is used<sup>[1]</sup>.

Heat transfer and flow structure in a packed bed are influenced by many parameters such as working fluid velocity, particle size, particle shape, particle density and thermo physical properties of particle and working fluid. Most of studies in packed bed investigated the effect of one or more of these parameters.

Li et al.<sup>[2]</sup> investigated experimentally the variation of particle shape on frictional pressure drops of fluid flow in porous beds packed with non-spherical particles. The beds are 635 mm

tall and 90 mm in diameter and packed with glass spheres 1.5 / 3 / 6 mm diameter, glass hollow spheres 6\*1 mm (ball diameter \* hole diameter), stainless steel hollow spheres 6\*3 mm, stainless steel cylinder 3\*3 mm (diameter \* length) and stainless steel cylinder 3\*6 mm. It was found that the pressure drops in the packed beds with hollow spheres and cylindrical particles are much higher than the predictions of the Ergun equation if the diameters of the spheres and cylinders are employed in the equation. Thomeo et al.<sup>[3]</sup> conducted the influence of tube to particle diameter ratio and air mass flux on the heat transfer in packed bed of glass beads, cooled by the wall through which air percolated. Tube – to – particle diameter ratios ( $D/D_p$ ) ranged from 1.8 to 55, while the air mass flux ranged from 0.204 to 2.422 kg/m<sup>2</sup>.s. The outlet bed temperature ( $T_L$ ) was measured by a brass ring – shaped sensor and by aligned thermocouples. The shape and average value of the entrance radial temperature profile depend on the particle size and fluid flow rate.

Also, the effect of Prandtl number of a medium on natural convection heat transfer across a horizontal layer was measured by [4] using stainless steel particles of diameters 1.6, 3.2 and 4.8 mm, glass particles of diameters 2.5 and 6 mm, and lead particles of diameter 0.95 mm with silicon oil, water and mercury as working fluids. The bed height varied from 2.5 to 12 cm, the experimental data indicate that the Prandtl number has a significant effect on the magnitude of the heat transfer across a differentially heated fluid saturated porous layer, especially for low values of the Prandtl number.

In this paper, forced convection heat transfer of air in porous rectangular channel which consist of sphere bead is investigated numerically. The effects of fluid velocity, particle diameter, constant heat flux imposed on rectangular channel and type of porous media (thermal conductivity) on the convection heat transfer, pressure drop and heat transfer enhancement are investigated.

## 2. Mathematical Problem

### 2.1. System Considered

The system under analysis shown in Fig.(1) is a rectangular duct (0.2m\*0.2m) cross section and

(1m) length that is completely filled randomly with a porous medium. The walls of the duct are maintained at constant heat flux. The porous medium has initially a uniform temperature (20°C). Four packing material, having different thermal conductivity have been employed with air as the working fluid.

**Table 1,**  
**Particle Thermal Conductivity of the Packing Materials Used in This Paper [5].**

Material	Aluminum	Alumina	Glass	Nylon
K	200	40	1.01	0.23
(W/m.K)				

The sphere pad inserts with different diameters and thermal conductivity taken from Ref. [5] are shown in Table (2). The other factors investigated are inlet air velocity which varies from (0.07 m/s) to (0.32 m/s), pad porosity (0.366 – 0.414) and duct constant heat flux varies at the range (1000 W/m<sup>2</sup>) to (3000 W/m<sup>2</sup>). Under these conditions heat transfer occurred by forced convection from heated duct walls into air passes through packed duct.

**Table 2,**  
**Particle Diameter, Heat Flux and Inlet Velocity Investigated.**

Material	D <sub>p</sub> (m)	Porosity	K <sub>s</sub> /K <sub>f</sub>	Heat flux (W/m <sup>2</sup> )	Inlet velocity (m/s)
Aluminum	0.03	0.938	7843.1	1000	0.07
	0.05	0.409		2000	0.19
	0.07	0.414		3000	0.32
Alumina	0.01	0.366	1568.6	1000	0.07
	0.03	0.398		2000	0.19
	0.05	0.409			
	0.07	0.414		3000	0.32
Glass	0.01	0.366	39.6	1000	0.07
	0.03	0.398		2000	0.19
	0.05	0.409			
	0.07	0.414		3000	0.32
Nylon	0.01	0.366	9	1000	0.07
	0.03	0.398		2000	0.19
	0.05	0.409			
	0.07	0.414		3000	0.32

## 2.2. Basic Equations

The flow field and temperature field are symmetrical above the centre line of the channel. The mathematical analysis carried out under the following assumptions [7]:

1. The flow is steady, fully developed and velocity is function of “y” cooled only.
2. Air and porous medium is in local thermodynamic equilibrium.
3. The permeability and porosity are functions of “y” coordinate only.
4. Thermal dispersion of heat in the x – direction is negligible into the energy equation.
5. All physical properties of the air and solid packing are constant and they will be calculated at the inlet condition.

The governing equations under the above assumptions are:

### a. Momentum Equation:

$$\frac{dp}{dx} = \frac{d^2u}{(y) dy^2} - \frac{u}{k(y)} - A(y)u^2 \quad \dots(1)$$

This equation known as “Darcy – Forchheimer – Brinkman momentum equation”, take into account the boundary effects and inertial forces of air through packed duct [7].

$$\varepsilon(y) = \varepsilon_o [1 + C \exp(\frac{d}{D_p} (-a))] \quad \dots(2)$$

Where “C” and “d” are empirical constants, “a” is the half width of the duct, “Dp” is the particle diameter and  $\varepsilon_o$  is the core porosity.

The permeability of porous medium is [8]:

$$k(y) = \frac{D_p^2 \varepsilon(y)^3}{175(1-\varepsilon(y))^2} \quad \dots(3)$$

The parameter A(y) is called the forchheimer constant [7]:

$$A(y) = \frac{1.75(1-\varepsilon(y))}{(y)^3 D_p} \quad \dots(4)$$

The boundary condition on velocity and pressure are:

$$\left. \begin{aligned} u = 0 & \quad \text{at } y = 0 \\ du/dy = 0 & \quad \text{at } y = w/2 \\ p = p_o & \quad \text{at } x = x_o \end{aligned} \right\} \quad \dots(5)$$

$$F_2 = \frac{\varepsilon(y)A(y)\rho}{\mu} (\Delta y)^2 \quad \dots(14)$$

### b. Continuity equation:

$$\frac{du}{dx} = 0 \quad \dots(6)$$

### c. Energy equation:

$$\rho C_p u \frac{dT}{dx} = k_e \frac{d^2 T}{dy^2} \quad \dots(7)$$

with the boundary condition:

$$\left. \begin{aligned} \frac{dT}{dy} = -\frac{q}{K_e} & \quad \text{at } y = 0 \\ \frac{dT}{dy} = -\frac{q_{loss}}{K_e} & \quad \text{at } y = w \\ T = T_i & \quad \text{at } x = 0 \end{aligned} \right\} \quad \dots(8)$$

The effective thermal conductivity ( $K_e$ ) is divided into ( $K_{st}$ ) stagnant thermal conductivity and ( $K_d$ ) thermal dispersion conductivity due to air flow through packed duct [5].

$$K_e = K_{st} + K_d \quad \dots(9)$$

$$K_{st} = K_f \left\{ 1 - \sqrt{1 - \varepsilon} + \frac{2\sqrt{1 - \varepsilon}}{1 - \lambda \beta} * \left[ \frac{(1 - \lambda)\beta}{(1 - \lambda\beta)^2} \ln\left(\frac{1}{\lambda\beta}\right) - \frac{\beta + 1}{2} - \frac{\beta - 1}{1 - \lambda\beta} \right] \right\} \quad \dots(10)$$

where  $\beta = 1.25 \left[ \left( 1 - \frac{(1 - \varepsilon)}{\varepsilon} \right)^{\frac{10}{9}} \right]$

and  $\lambda = \frac{K_f}{K_{st}}$

$$K_d = 0.1 k_f P_{ep} \quad \dots(11)$$

## 3. Numerical Method

A finite differences method with central differencing scheme shown in Fig.(2) is used for the numerical solution of the problem, including a line – by – line triadiagonal matrix algorithm (TDMA) method for solving the set of algebraic equation that is yielded from the initial guess of the velocity distribution and boundary conditions. momentum Equation (1) is rewritten in a different form as:

$$0 = u_{ij+1} - u_{ij} (F_1 + F_2 u_{ij}) + u_{ij-1} + F_3 \quad \dots(12)$$

where:

$$F_1 = 2 + \frac{\varepsilon(y)}{K(y)} (\Delta y)^2 \quad \dots(13)$$

$$F_3 = \left( \frac{p_o - p_L}{L} \right) \frac{\varepsilon(y)}{\mu} (\Delta y)^2 \quad \dots(15)$$

and Energy Equation (7) is rewritten as:

$$0 = T_{i,j+1} + T_{i,j-1} + (F4 - 2) T_{i,j} + T_{i-1,j} \quad \dots(16)$$

where:

$$F4 = \frac{\rho c_p u (\Delta y)^2}{K_e (\Delta x)} \quad \dots(17)$$

The momentum equation is solved to determine the velocity profile, then, the velocity field is combined with the energy equation to determine the temperature profile.

After knowing the temperature distribution inside the duct bulk temperature ( $T_b$ ) can be found from:

$$T_b(x) = \frac{\int_A u T dA}{\int_A u dA} \quad \dots(18)$$

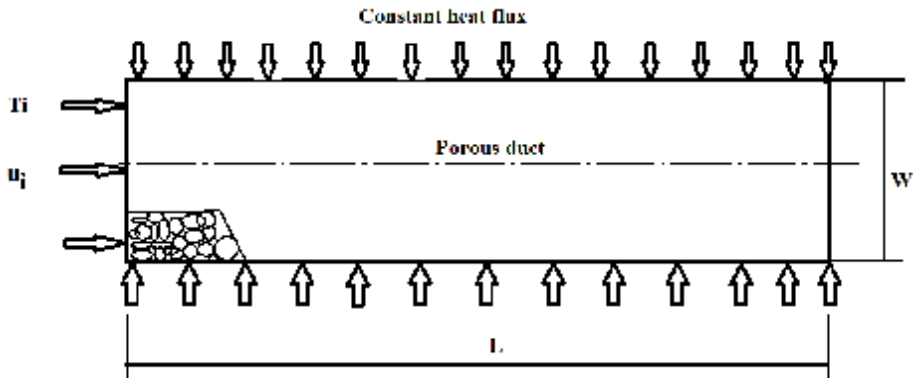


Fig. 1. Physical Model

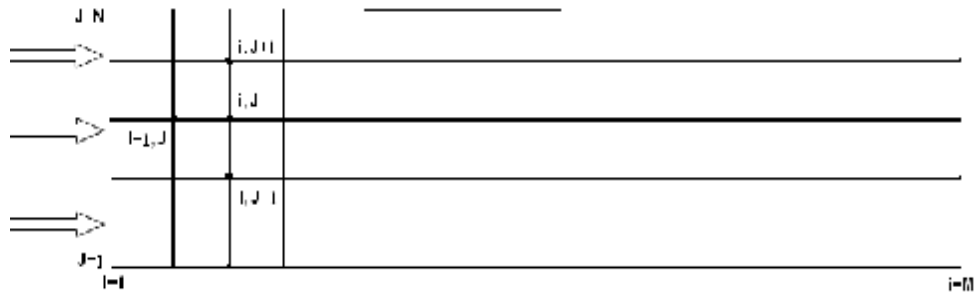


Fig. 2. Coordinate System and Grid Distribution.

The convection heat transfer coefficient ( $h$ ) in packed duct can be found from:

$$h = \frac{Q_w}{T_s - T_b} \quad \dots(19)$$

Nusselt number ( $Nu$ ) can be expressed according to thermal conductivity of the fluid and equivalent diameter of the duct as:

$$Nu = h \frac{d_{eq}}{K_f} \quad \dots(20)$$

Reynolds number ( $Re_\epsilon$ ) is based on particle diameter and porosity as:

$$Re_\epsilon = \frac{u D_p}{\gamma (1-\epsilon)} \quad \dots(21)$$

Also, pressure drop ( $\Delta p / L$ ) through packed duct for Reynolds number higher than (10) can be found as [ 9]:

$$\frac{\Delta p}{L} = 1.75 \frac{(1-\epsilon) \rho U^2}{\epsilon^3 D_p} \quad \dots(22)$$

#### 4. Results and Discussion

The present analysis is confined to studying the influence of pad conductivity, particle diameter, inlet velocity and heat flux on forced convection in porous duct. Table (1) shows the range of the variables used in the numerical calculation. A total of (144) runs were conducted

to cover four packed bed material (Aluminum, Alumina, Glass and Nylon) with four particles diameter ( 1,3,5 and 7 cm). The range of heat flux used varied from ( $1000 \text{ W/ m}^2$ ) to ( $3000 \text{ W/ m}^2$ ) and inlet air velocity varied from (0.07 to 0.32 m/s).

The velocity profile, pressure drop, temperature profile, variation of air temperature along the duct, local heat transfer coefficient, local Nusselt number and average Nusselt number were investigated in this paper with the parameters illustrated in Table (1).

#### 4.1. Velocity Profile

Fig.(3) shows the axial velocity profile for (0.07, 0.19 and 0.32 m/s), the variation in velocity occur near the duct wall due to the no homogeneity in porosity and wall channeling effect, while the velocity is constant at the duct core. It can see the channeling increases with decreases particle diameter.

#### 4.2. Pressure Drop

Fig.(4) shows the pressure gradients of air flow through beds packed by sphere particles with diameter (1,2,3,5 and 7 cm). It is found that the pressure drop decreased with increasing particle diameter and the particle conductivity have no effect on pressure drop through the bed.

#### 4.3. Temperature Profile

In general, the variation of temperature distributions across the duct affected by heat flux, Reynolds number, particle diameter and particle conductivity. The general shape of all curves obtained, shown that the high porosity near the wall leading to enhancement of heat transfer from heated duct surface to air which passes faster in this region due to channeling effect and the air temperature gradually decrease going away from the duct wall.

Figs.(5),(6),(7) and (8) represent similar plots of axial temperature profiles of air for (Aluminum, Alumina, Glass and Nylon particle), ( $D_p = 3,5$  and 7 cm), ( inlet air velocity = 0.32 m/s) and ( heat flux =  $1000 \text{ W/ m}^2$ ). The temperatures are plotted as a function of axial position, at the entrance of duct the variation of temperature taken approximately (4 cm) from the wall while the variation taken all width at the duct exit. Fig.(9) illustrate temperature distribution for four type of packing at 0.32 m/s inlet velocity,

$1000 \text{ W/ m}^2$  heat flux and 3 cm particle diameter. It is seen that Aluminum and Alumina plots decrease gradually from duct surface into duct centerline. The variation in Glass and Nylon plots taken place at small region near the surface, not extend into bulk region. The mechanisms of heat transfer in packed bed are convective heat transfer from duct wall to the air, convective heat transfer from the packing particles to the air and conduction from the wall to the particles. In Aluminum and Alumina plots which have high conductivity enhance conduction from wall to the particles and increased particle temperature then increased convective heat transfer from packing particles to the air.

#### 4.4. Local Heat Transfer Coefficient

Fig. (12) shows local heat transfer coefficient in packed duct for Aluminum, Alumina, Glass and Nylon packing. It is concluded that for a constant thermal conductivity an increase in particle size yields a decrease in porosity and contact area between pad and air then decrease in local heat transfer coefficient. Any increasing in inlet velocity yields to increase turbulence and decrease thermal boundary layer thickness which cause high local heat transfer coefficient for a constant particle size, packing conductivity and heat flux, this result is plotted in fig.(13) for 4 – packing. Fig.(14) illustrate the effect of heat flux on local heat transfer coefficient. It is seen that ( $h_x$ ) increase as heat flux increase, due to high temperature difference between duct wall temperature and air bulk temperature.

#### 4.5. Local Wall to Fluid Nusselt Number

Aluminum, Alumina, Glass and Nylon packing evaluated by Eq.(20) using equivalent diameter of duct and air thermal conductivity are drawn in Fig.(15) and Fig.(16) which show that the plots have similar trend of ( $h_x$ ), increased at (5.1, 4.3, 2.2 and 1.4 percent) with increasing heat flux and at (36.7,38.8,44.6 and 45.7 percent) inlet air velocity but ( $Nu_x$ ) increased at (12.8,12.6,8.3 and 5.8 percent) with decreasing particle size. For (Aluminum, Alumina, Glass and Nylon) packing respectively the variation of ( $Nu_x$ ) with duct length for 4 – packing are presented for (heat flux =  $1000 \text{ W/ m}^2$ , inlet velocity = 0.32 m/s and particle diameter =3 cm) in Fig. (17). It show the highest ( $Nu_x$ ) for Aluminum packing due to high thermal conductivity which results in high contact

conduction then ( $Nu_x$ ) of Alumina, Glass and Nylon respectively.

#### 4.6. Average Nusselt Number Versus Particle Reynolds Number

The relationship between average Nusselt ( $Nu_{av}$ ) and particle Reynolds number ( $Re_p$ ) is plotted in Fig.(18) for 4-packing materials used in this paper. The relationship is correlated in the form:

$$Nu_{av} = C (Re_p)^m \quad \dots (23)$$

Table (3) summarizes the correlation constants (C) and (m) for all the packing materials. In general, the exponent (m) tends to decrease with increasing thermal conductivity of the packing material but the factor (C) increase with increasing it.

**Table 3,**  
**Constant (m & C) for Eq.(23).**

Packing material	C	m
Aluminum	87.54	0.0838
Alumina	68.692	0.0951
Glass	29.08	0.1339
Nylon	17.949	0.1473

A comparisons of final results of average Nusselt number for 4-packing material are presented in Table (4). It is observed that Aluminum ( $Nu_{av}$ ) is about (0.85), (2.2) and (3.1) times approximately higher than Alumina, Glass and Nylon respectively

#### 4.7. Optimization Heat Transfer and Pressure Drop

The results show that heat transfer increased as particle diameter decreased and inlet velocity increased which proceeded high pressure drop through the packed duct. A good design of packed bed must have an optimization between pressure drop and heat transfer. For that ( $Nu_{av} / \Delta p$ ) parameter is used to analyze the results of 4-packing involved in this paper. It is shown that the finest ratio obtained is (19.12) at ( $D_p = 7\text{cm}$ , inlet velocity = 0.07m/s and heat flux = 3000 W/m<sup>2</sup>), (18.96) and (18.5) at the same variable but (heat flux = 2000 and 1000 W/m<sup>2</sup>) respectively when using Aluminum as packing material.

**Table 4,**  
**Comparison Between Average Nusselt Number for 4 – Packing Material.**

$D_p$ (cm)	$N_{u\ av}$				Pressure $P_{a/m}$	Inlet velocity VEL m/s
	Aluminum	Alumina	Glass	Nylon		
1	199.948	171.466	96.111	64.276	1619.45	0.32
2	183.1598	157.917	90.663	61.745	397.43	0.32
5	178.1	153.806	88.962	60.937	216.736	0.32
7	176.063	162.713	88.292	60.627	148.028	0.32
1	207.906	177.194	97.73	951.64	1619.45	0.32
3	189.75	158.337	92.0927	62.364	397.43	0.32
5	184.31	156.55	90.333	61.539	216.736	0.32
7	182.075	164.107	89.629	61.217	148.028	0.32
1	210.776	179.23	98.292	65.1804	1619.45	0.32
4	192.119	159.93	92.582	62.57	397.43	0.32
5	186.533	158.095	90.802	61.742	216.736	0.32
7	184.217	156.2	90.087	61.416	148.028	0.32
1	169.86	144.133	79.255	53.115	583.004	0.19
3	154.62	132.117	74.738	51.06	143.075	0.19
5	150.055	128.488	73.32	50.398	78.025	0.19
7	148.092	126.946	72.737	50.131	53.29	0.19
1	175.888	148.398	80.428	53.604	583.004	0.19
3	159.568	135.66	75.77	51.508	143.075	0.19
5	154.69	131.83	74.311	50.833	78.025	0.19
7	152.58	130.181	73.703	50.55	53.29	0.19
1	178.049	149.909	80.831	53.769	583.004	0.19
3	161.33	136.91	76.122	51.66	143.075	0.19
5	156.384	133.005	74.649	50.98	78.025	0.19
7	154.173	131.317	74.033	50.703	53.29	0.19

1	128.468	106.313	53.649	35.093	64.778	0.07
3	115.324	96.077	50.316	33.705	15.89	0.07
5	111.382	93	49.272	33.249	8.669	0.07
7	109.57	91.591	48.8035	33.049	5.9211	0.07
1	132.192	108.82	54.252	35.3344	64.778	0.07
3	118.296	98.113	50.842	33.926	15.89	0.07
5	114.147	94.904	49.774	33.46	8.669	0.07
7	112.239	93.128	49.294	33.26	5.9211	0.07
1	133.517	109.707	54.458	35.416	64.778	0.07
3	119.347	98.826	51.022	34.0008	15.89	0.07
5	115.153	98.569	49.946	33.536	8.669	0.07
7	113.192	94.069	49.461	33.3319	5.9211	0.07

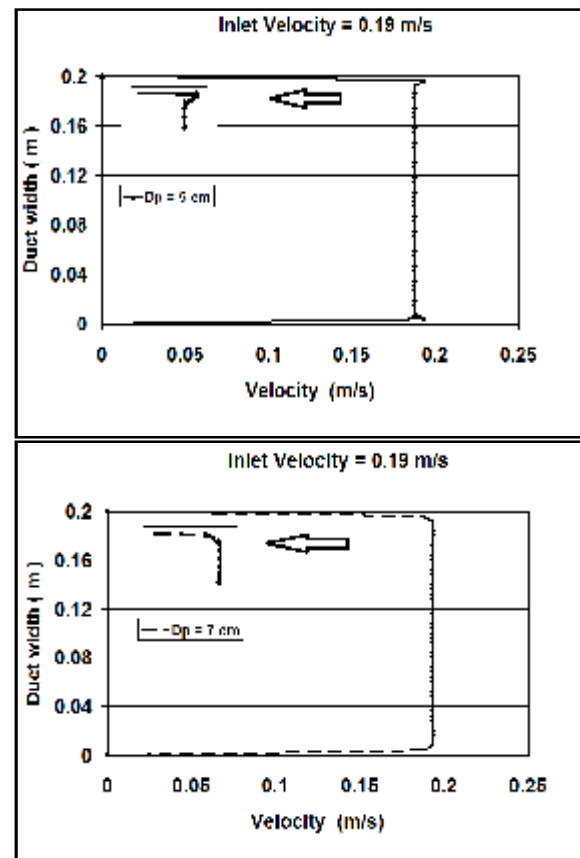
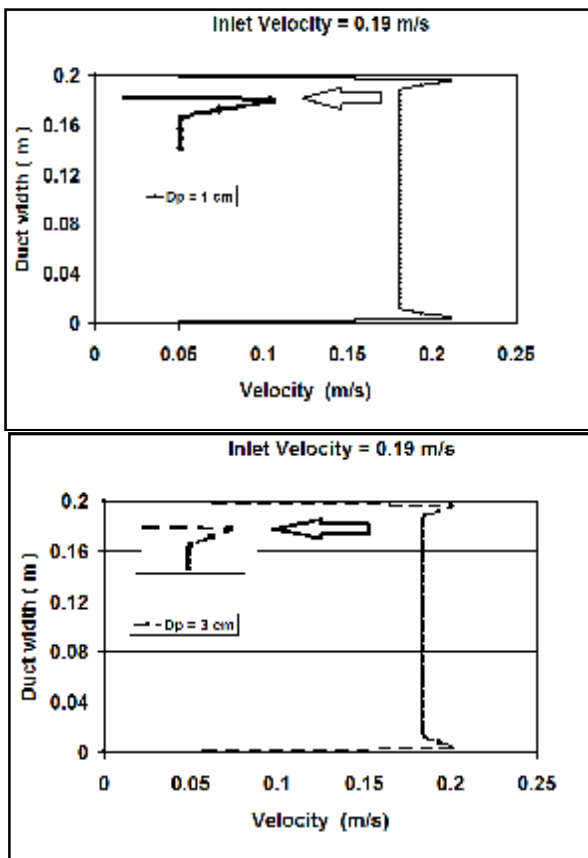


Fig. 3. Velocity Profile in Packed Duct.



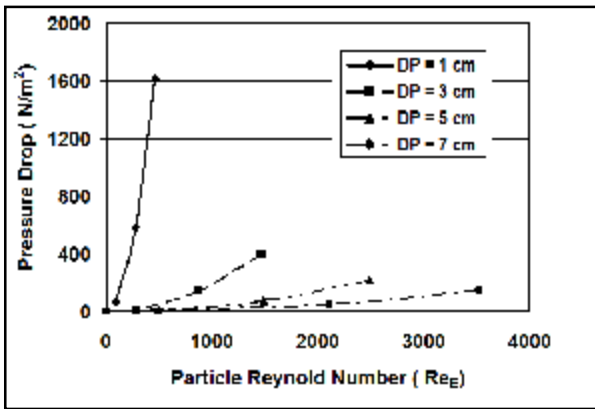


Fig. 4. Pressure Drop Versus Particle Reynolds Number.

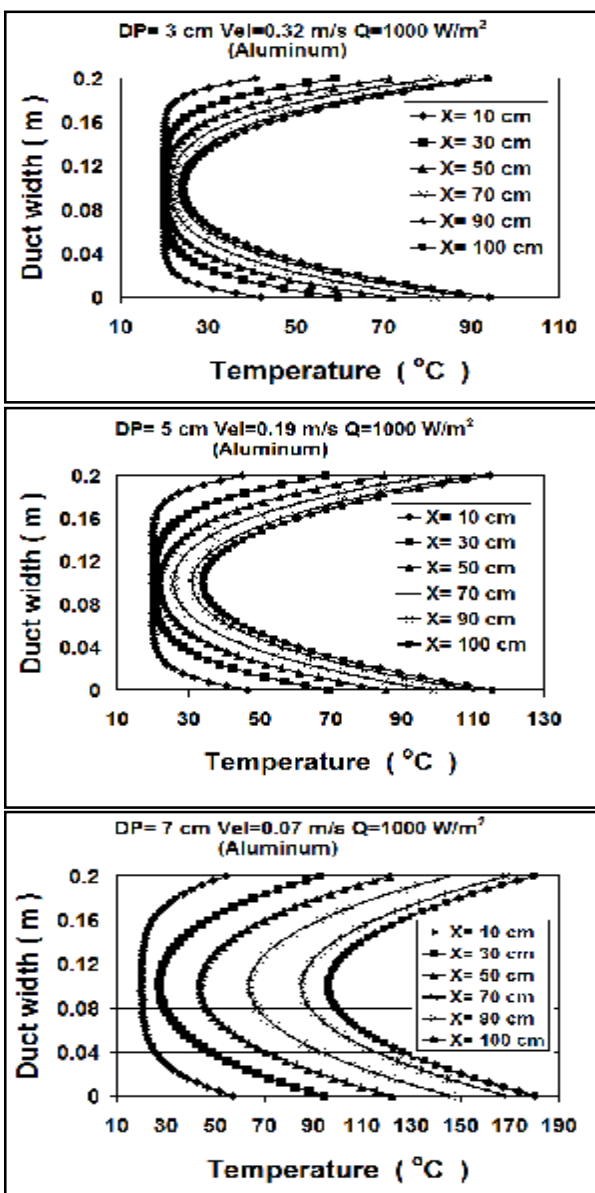


Fig . 5. Temperature Profile Versus Duct width for Various Particle Sizes for Aluminum Packing.

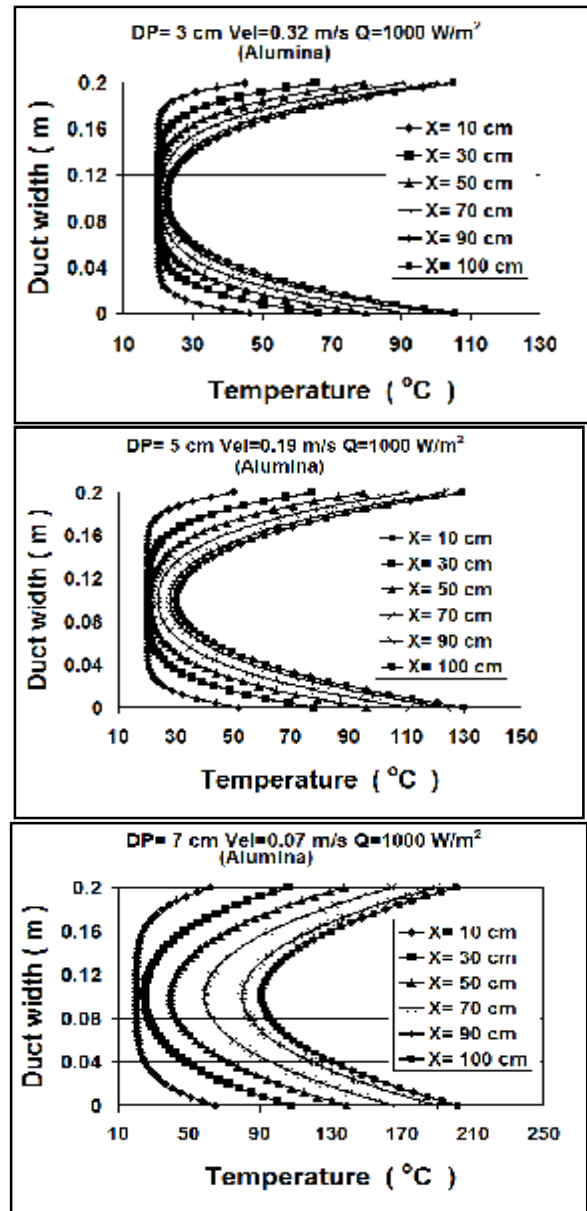
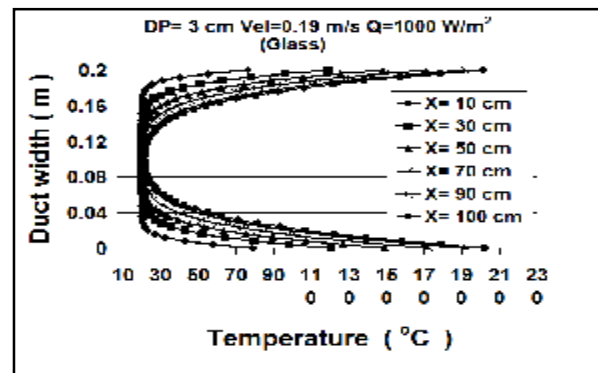


Fig. 6. Temperature Profile Versus Duct Width for Alumina Packing.



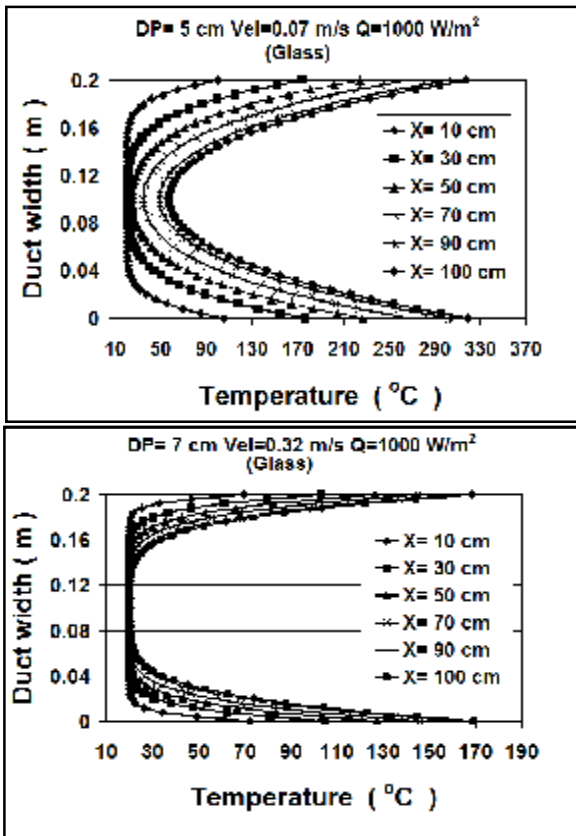


Fig. 7. Temperature Profile Versus Duct Width for Glass Packing.

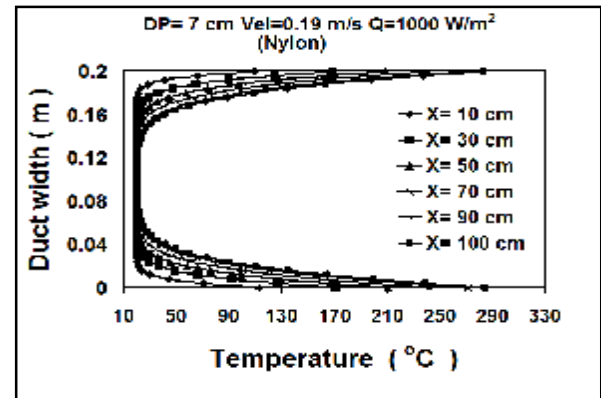


Fig. 8. Temperature Profile Versus Duct Width for Nylon Packing.

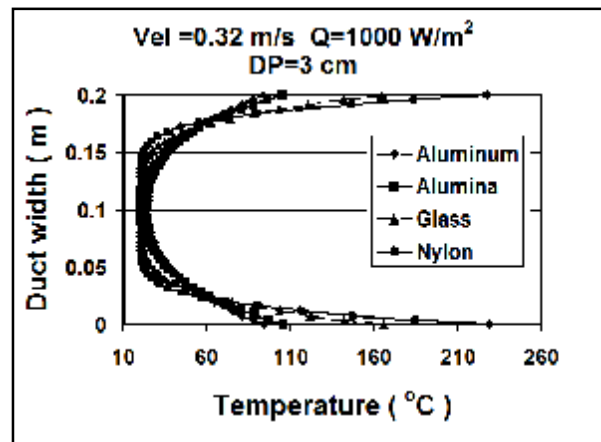
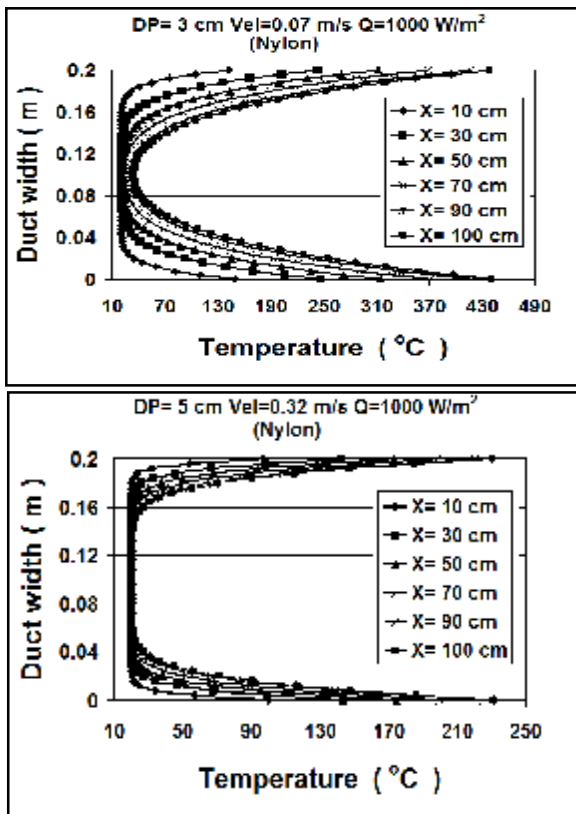


Fig. 9. Temperature Profile Versus Duct width for 4-Packing Material Width for Different Heat Flux.



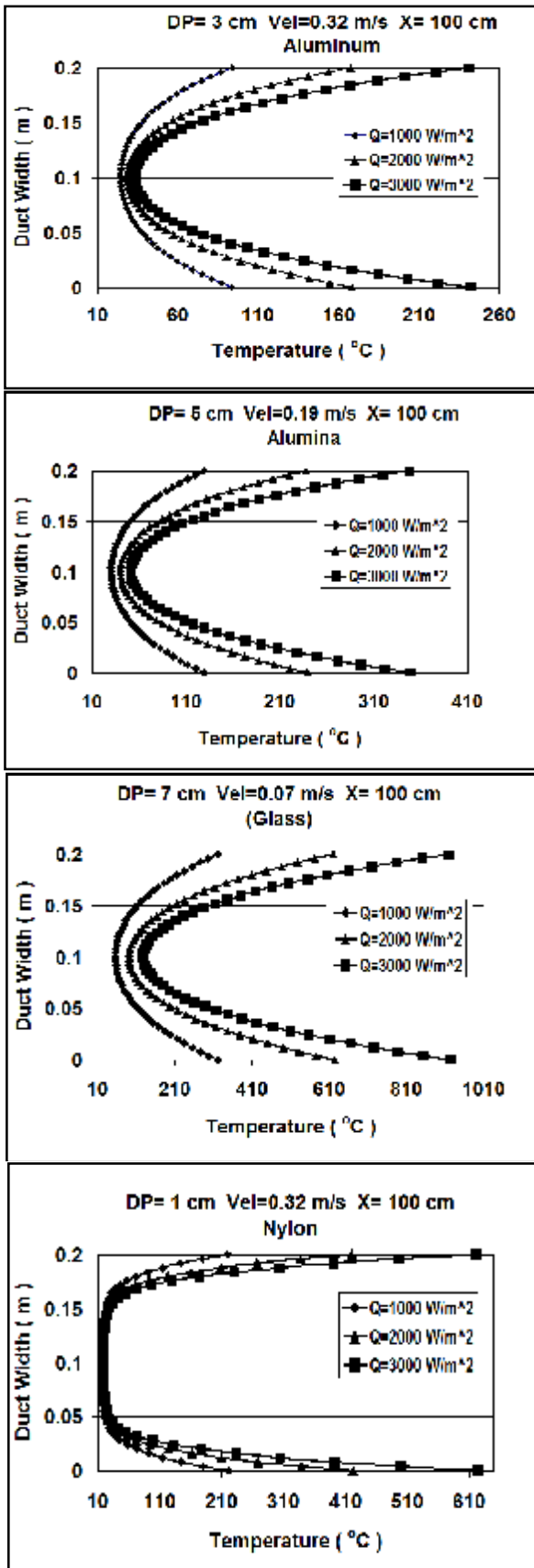


Fig. 10. Temperature Profile Versus Duct.

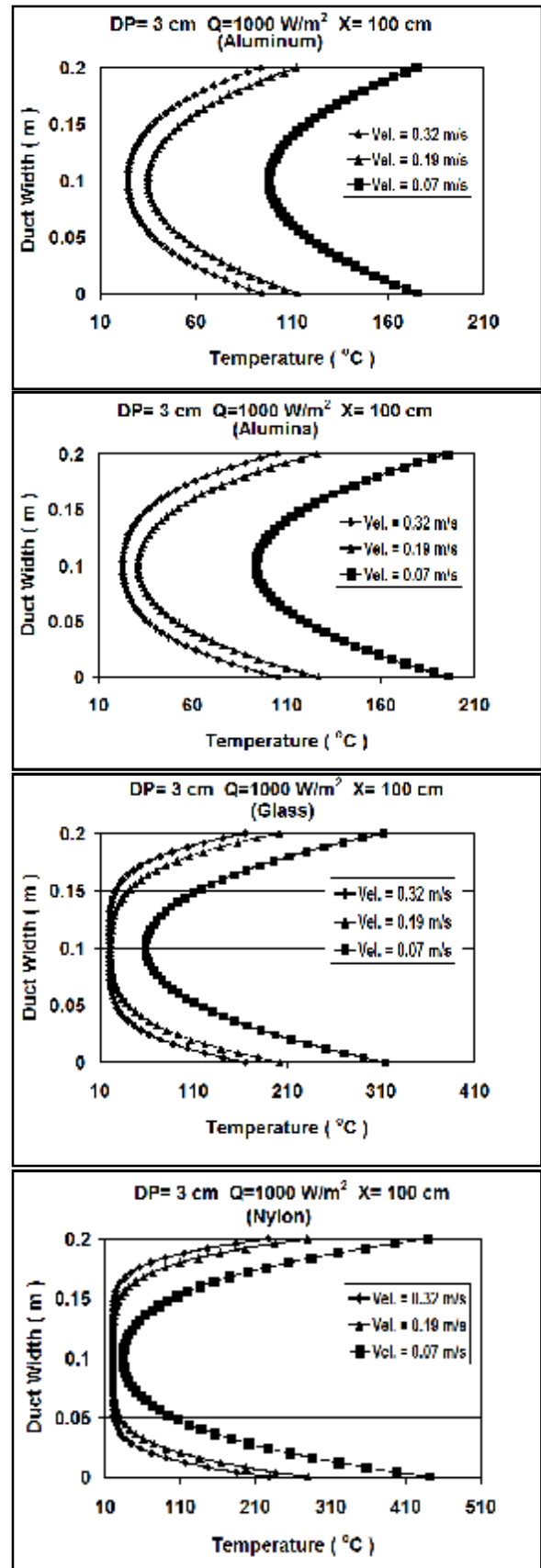


Fig. 11. Temperature Profile Versus Duct Width for Different Inlet Velocity.

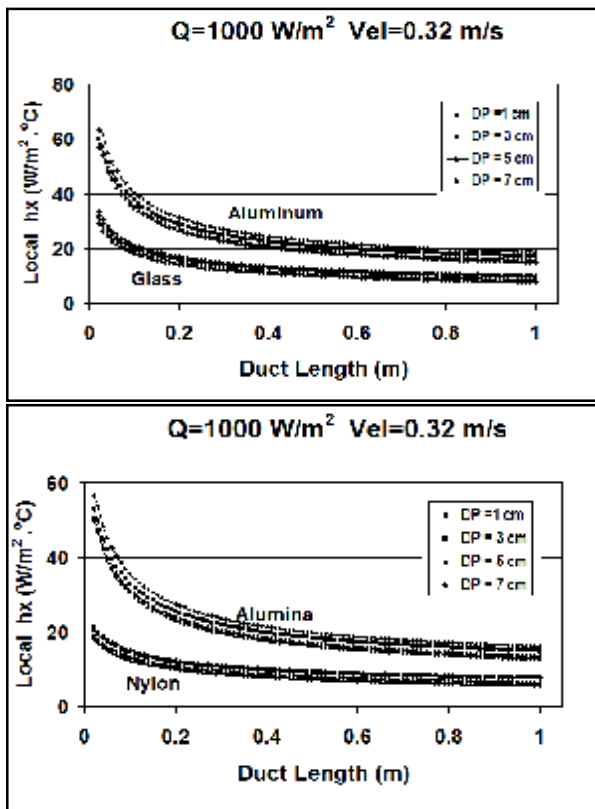


Fig. 12. Local Heat Transfer Coefficient Versus Particle Size for 4-Packing.

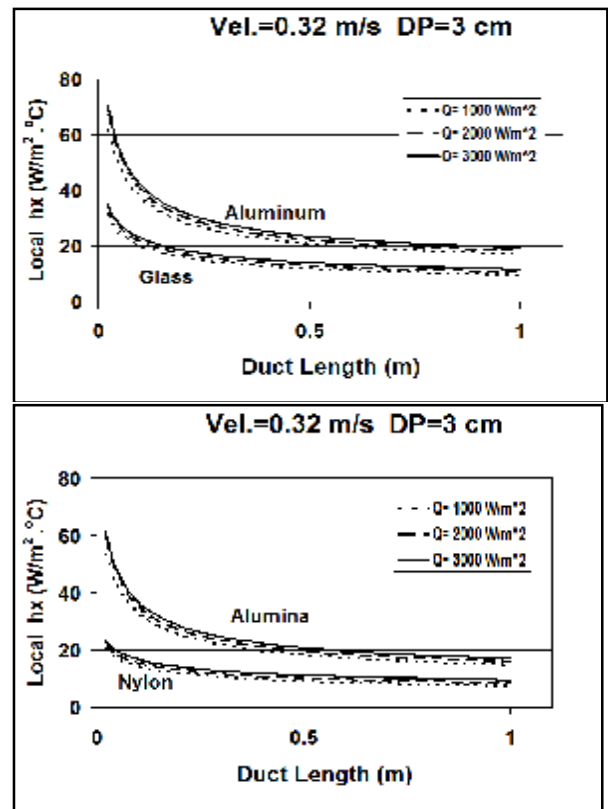


Fig. 14. Local Heat Transfer Coefficient Versus Heat Flux for 4-Packing.

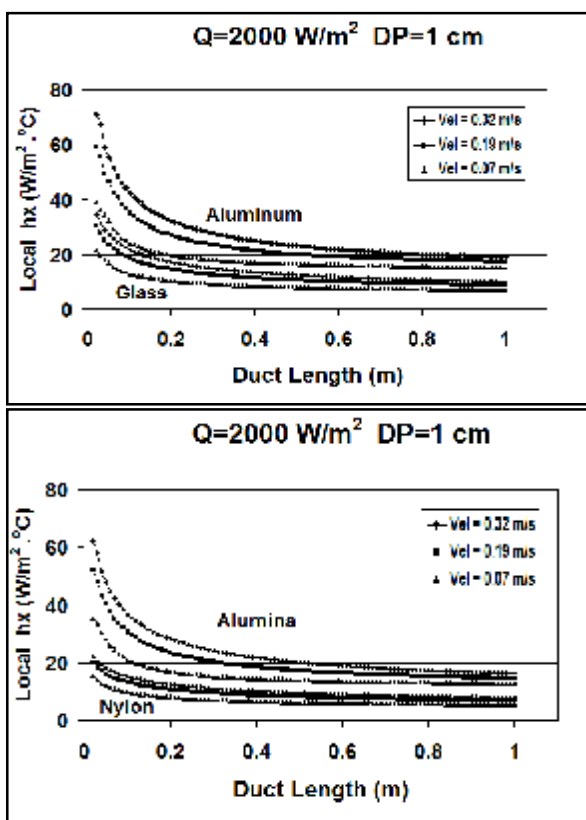


Fig. 13. Local Heat Transfer Coefficient Versus Inlet Velocity for 4-Packing.

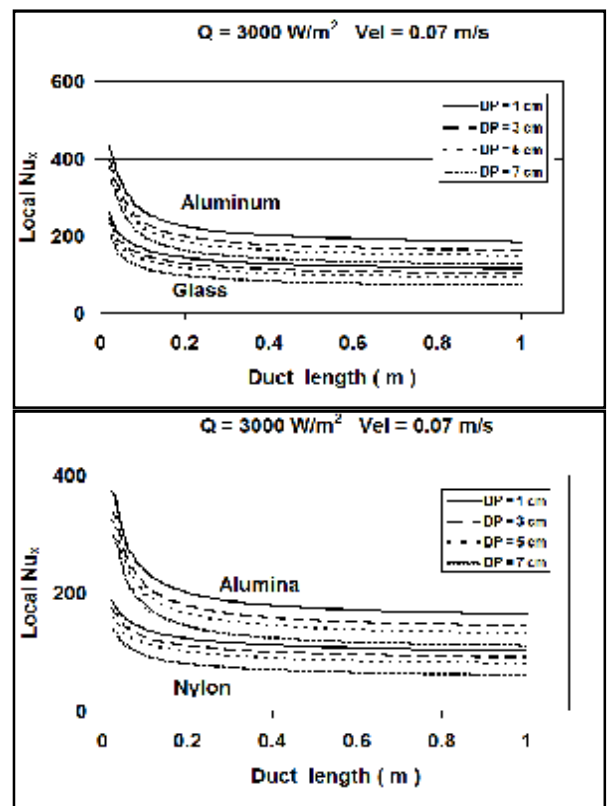


Fig. 15. Local Nusselt Number Versus Particle Size for 4-Packing.

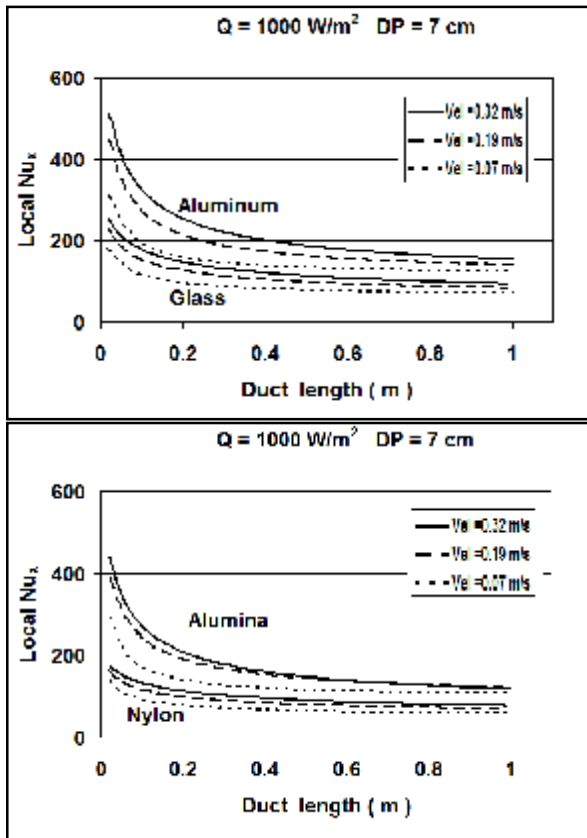


Fig. 16. Local Nusselt Number Versus Inlet Velocity for 4-Packin.

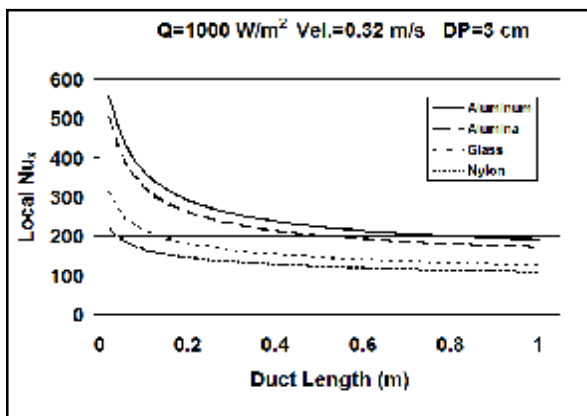


Fig. 17. Local Nusselt Number Versus Ductwidth for 4-Packing Material.

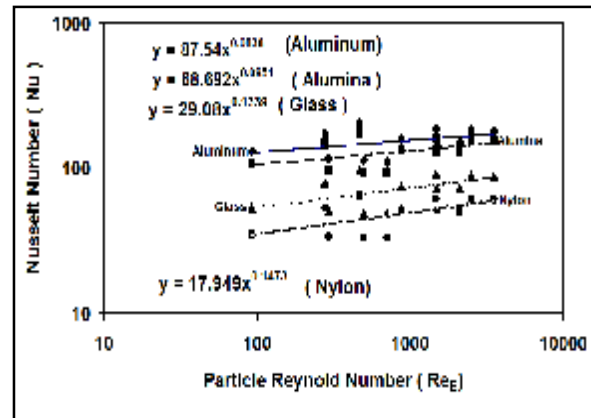


Fig. 18. Correlation of Nusselt Number and Particle Reynolds Number.

### 5. Conclusions

In this paper, various effect on forced convection heat transfer and pressure drop in packed duct are investigated numerically using 4-packing material (Aluminum, Alumina, Glass and Nylon). It is shown that:

1. Average Nusselt number ( $Nu_{av}$ ) increased with increasing packing conductivity, Aluminum ( $Nu_{av}$ ) is higher about (0.85, 2.2 and 3.1 times) than Alumina, Glass and Nylon respectively.
2. ( $Nu_{av}$ ) increased with decreasing particle size, but this result high pressure drop. For good design, it is found that the finest ratio ( $Nu_{av} / \Delta p$ ) is (19.12) when Aluminum is packing material, particle diameter = 7cm, inlet velocity = 0.07 m/s and heat flux = 3000W/m<sup>2</sup>.
3. ( $Nu_{av}$ ) increased with increasing inlet air velocity and heat flux supplied into duct walls.
4. Many correlation are obtained for ( $Nu_{av}$ ) as a function of ( $Re \epsilon$ ) which included the effects of particle size, velocity, heat flux and packing conductivity.

### Nomenclature

A	Duct cross – section area	m <sup>2</sup>
A(y)	Forchheimer constant	--
Cp	Air specific heat at constant pressure	kJ/kg.K
Dp	Particle diameter	cm
d <sub>eq</sub>	Duct equivalent diameter	m
dp/dx	Pressure gradient	Pa/m
h <sub>x</sub>	Local heat transfer coefficient	W/m <sup>2</sup> .K

i	Index for axial direction	--
j	Index for vertical direction	--
K(y)	Permeability of porous medium	--
K <sub>f</sub>	Fluid thermal conductivity	W/m.K
K <sub>s</sub>	Particle thermal conductivity	W/m.K
K <sub>e</sub>	Effective thermal conductivity	W/m.K
K <sub>st</sub>	Stagnant thermal conductivity	W/m.K
K <sub>d</sub>	Thermal dispersion conductivity	W/m.K
L	Duct length	m
p <sub>o</sub>	Pressure at exit duct	Pa
q	Heat absorbed by air	W
Q <sub>w</sub>	Heat flux	W
T	Temperature	°C
T <sub>i</sub>	Inlet temperature	°C
T <sub>b</sub>	Air bulk temperature	°C
T <sub>s</sub>	Surface duct temperature	°C
U <sub>i</sub>	Velocity at duct entrance section	m/s
W	Duct width	m
Y	Index vertical length (width)	m
Re <sub>e</sub>	Particle Reynolds number	--
Nu <sub>x</sub>	Local Nusselt number	--
Nu <sub>av</sub>	Average Nusselt number	--
Pe <sub>d</sub>	Particle Peclet number	--
ρ	Density	kg/m <sup>3</sup>
μ	Dynamic viscosity	kg/m.s
γ	Kinematic viscosity	m <sup>2</sup> /s
ε	Porosity	--
ε(y)	Porosity with respect to vertical location	--

- [3] with Non – Spherical Particles”, *Transp. Porous Med.*, Volume 89, Page 35 – 48, 2011.
- [4] Thomeo J., Rouiller C. and Freire J.,” *Experimental Analysis of Heat Transfer in Packed Beds with Air Flow*”, *Ind. Eng. Chem. Res.*, Volume 43, Page 4140 – 4148, 2004.
- [5] Jonson T. and Catton I.,” *Prandtle Number Dependence of Natural Convection in Porous Media*”, *Journal of Heat Transfer*, Volume 109, Page 371 – 377, 1987.
- [6] Naser K., Ramadhyani S. and Vistanta R.,” *An Experimental Investigation on Forced Convection Heat Transfer from Cylinder Embedded in a Packed Bed*”, *Journal of Heat Transfer*, Volume 116, Page 73 – 79, 1994.
- [7] Chandrasekhara B. and Radha N.,” *Effect of Variable Porosity on Laminar Convection in a Uniformly Heated Vertical Porous Channel*”, *Wärme – und Stoffübertragung*, Volume 23, Page 371 – 377, 1988.
- [8] Hong J., Yamada Y. and Tien C., “ *Effects on Non – Daracian and Non uniform porosity on Vertical Plate Natural Convection in Porous Media*”, *Transactions of the ASME*, Vol. 109, pp 356 – 376, 1987.
- [9] Hwang G. and Chao C., “ *Heat Transfer Measurement and Analysis for Sintered Porous Channels*”, *Transactions of the ASME, J. Heat Transfer*, Volume 116, pp. 456 – 464, 1994.
- [10] Vafai K.,” *Handbook of Porous Media*”, 2nd Edition by Taylor & Franice Group, 2005.

## 6. References

- [1] Petrov A.S,” *Momentum and Heat Transfer in a Packed Bed*”, MAE / CENG221A,2006.
- [2] Li L. and Ma W., “ *Experimental Study on the Effective Particle Diameter of a Packed Bed*

## تأثير خصائص الحشوة الكروية على انتقال الحرارة وفقدان الضغط في مجرى مسامي

مثنى لطيف عبد الله

سلمان حسين عمران

كفاح حامد هلال

قسم الميكانيك/ معهد التكنولوجيا - بغداد

## الخلاصة

اجريت في هذا البحث دراسة عديدة لتأثير قطر الجزيئة المكونة للحشوة المسامية والموصلية الحرارية لها وسرعة الهواء الداخل على انتقال الحرارة بالحمل القسري خلال مجرى مسامي مسخن بفيض حراري ثابت. أربعة أنواع من الحشوات مصنوعة من ( الالمنيوم، الالومينا، الزجاج والنايلون) ويمدى موصلية حرارية يتراوح بين  $0.23 \text{ W/m.K}$  للنايلون و  $200 \text{ W/m.K}$  للالمنيوم وبقطر جزيئة (1,3,5,7 cm) وسرعة (0.07, 0.19, 0.32 m/s) و بفيض حراري ثابت مقداره (1000,2000,3000  $\text{ W/m}^2$ ) تم اختبارها. لقد بينت النتائج ان انتقال الحرارة ( معدل رقم نسلت  $\text{Nu}_{av}$ ) تزداد بزيادة الموصلية الحرارية للحشوة المسامية وسرعة الهواء الداخل والفيض الحراري، ولكن يقل بزيادة قطر الجزيئة. معدل رقم نسلت ( $\text{Nu}_{av}$ ) لحشوة الالمنيوم أعلى ب (0.85, 2.2, 3.1 مرة) من ( الالومينا، الزجاج والنايلون) على التوالي. من المفاضلة بين انتقال الحرارة وفقدان الضغط خلال الحشوة المسامية، نجد أن أفضل نسبة ( $\text{Nu}_{av} / \Delta p$ ) تساوي (19.12) عند ( $U = 0.07 \text{ m/s}$ ,  $D_p = 7 \text{ cm}$ ) و فيض حراري ( $3000 \text{ W/m}^2$ )، واستخدام الالمنيوم كحشوة مسامية داخل المجرى.